Tiny Surface Defects on Small Ring Parts using Normal Maps

Yang Zhang[1], Jia Song[1], Huiming Zhang[1], Jingwu He[1] and Yanwen Guo[1,2(✉)]

[1] National Key Laboratory for Novel Software Technology,
Nanjing University, Nanjing, 210023, China
[2] Science and Technology on Information Systems Engineering Laboratory,
Nanjing, 210007,China
ywguo@nju.edu.cn

Abstract. Detection of tiny surface defects on small ring parts remains challenging due to the unnoticeable visual features of such defects and the interference of small surface scratches. This paper proposes a novel method for detecting tiny surface defects based on normal maps of metal parts. To better characterize features of tiny defects and differentiate them from small scratches, we recover the normal map of the metal part through analyzing its directional reflections obtained with our specifically designed directional light units. Based on the normal map, a cascaded detector trained by the AdaBoost approach combined with the joint features and fast feature pyramid is used to localize the defects, achieving fast and accurate detection of tiny surface defects. The proposed method can achieve high detection accuracy with extremely fast speed, only 23 milliseconds per metal part, and comparisons against other methods show our superiority.

Keywords: Defect detection; Tiny surface defect; Normal maps; Combined light units

1 Introduction

In recent years, with the development of machine vision and the extensive application of precision machining of metal parts, defect detection of small metal parts has gained increasing attention. Detection of tiny surface defects is serious to ensure the quality of mechanical parts. The defects of parts may affect the safety and performance of the entire product. In particular, some products require parts to be with high precision such as automotive parts for which defected parts may lead to car safety problems and large-scale car recalls. Therefore, in electronics, machinery and other related industries, detection of small metal parts faults (scratches, defects, etc.) is particularly important.

For a long time, defect detection is a complex and time-consuming job of engineers and inspectors, with low detection probability and a waste of manpower. Due to the continuing and rapid advances in both hardware and software technology of sensors such as the laser and camera, automatic detection system of surface defects has received considerable attention. In [1], the metal surface defects are detected by using the iterative thresholding technique. However, the algorithm only works well for those obvious

defects of metal surface. The length, width and depth of defects are predicted by the magnetic-leakage method [2]. Besides, a finite element method [3] is used to establish a model of laser ultrasonic transmission wave to detect the depth of surface defects and the relationship between characteristics of the transmitted wave and defect depth. The relationship between the acoustic surface waves and the defects of micro-cracks with different depths is used for defect detection [4]. As a rapidly developing defect detection technique, infrared thermography is used to estimate the depth of defects to detect defects [5]. However, those methods used to estimate defect depth are based on surface heating, which may damage the parts during inspection. Other methods based on the estimated depth are in [6] and [7]. Most of the existing depth estimation methods are introduced for subsurface defect detection of unknown depth in metal parts, and the feature information captured by various sensors is difficult to apply directly.

More and more defect detection algorithms based on machine learning are applied in the field of industrial testing [8], [9]. Compared with the methods relying on specific sensors such as laser and ultrasonic, using machine learning based visual detection to realize the detection of metal parts is not only accurate and efficient, but also with high reliability. In this paper, we apply this attractive technique to inspect the tiny surface defects on small ring parts. Given a metal part shown in Fig.1, the part with a deep scratch is deemed as a defected one, while a slight surface scratch is not a defect. For this part with the 3.5cm diameter, the depth of scratch exceeding 0.5mm is viewed as “deep” from the view of engineers.

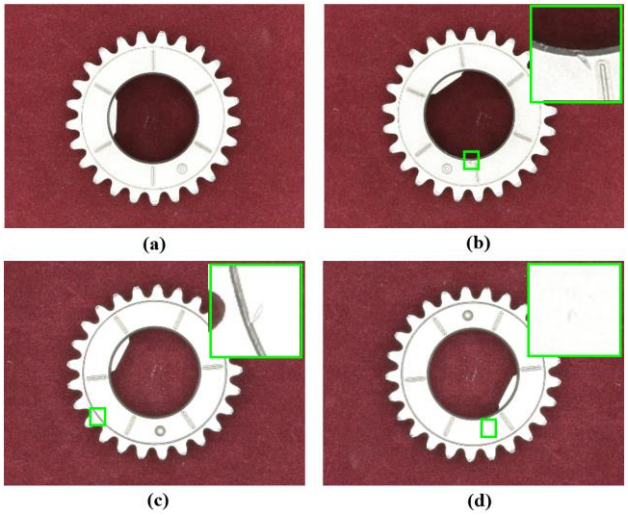

Fig. 1. Mechanical parts. (a) A normal part. (b-d) Parts with tiny surface defects. From the view of engineers, the scratch with over 0.5mm depth is considered as a defect.

It is challenging to perform such defect detection because the tiny defects can hardly be described with only simple visual features. Moreover, it is difficult to differentiate such defects from small surface scratches due to manufacturing technology, considering only the visual appearance. To deal with these problems, our key insight is to explore

the geometry feature of the metal part using the recovered normal map, and then process them by machine learning to identify whether there is any visual defect on metal surface. The proposed visual detection method contains two core components: normal map recovery based on directional reflections and a defect classifier using the recovered normal maps. Experiments demonstrate that the proposed method can be effectively applied to the detection of tiny surface defects with high detection accuracy and fast speed.

The rest of the paper is organized as follows. Section 2 is an overview of our detection framework. Section 3 introduces the reconstruction of the normal map of a metal part. Section 4 explains the diagram of normal information extraction and detection of tiny surface defects. The experimental results and analysis are summarized in Section 5. Section 6 concludes this paper and describes the future work.

2 Overview

The proposed defect detection framework contains an image acquisition system and an image analysis module. Small metal parts images are first acquired by our image acquisition system, and then processed by image analysis to identify whether there are any visual defects on the metal surface.

2.1 Image acquisition system

We have designed an image acquisition system which uses a special device consisting of a shading box, a transparent conveyor belt, a CCD camera, and three sets of LED light units (top, middle, bottom). The output of our classifier mostly depends on the quality of the recovered normal map. Therefore, for better quality of the normal maps we need a way to estimate the normal maps accurately. As illustrated in Fig. 2(a), a shading box is designed to ensure a lighting-free, dark environment with black flannelette on the inner surface which can help relieve the influence of reflection of box surface. Specially, the LED lamps are installed around the platform which are above 20cm in order to make the lights shot the parts with an angle of 45 degrees.

In Fig. 2(a), the top and bottom light units comprise four LED light belts parallel to the moving direction of the conveyor belt respectively. The middle light units are arranged along with the four main directions (north, south, east, west) of the center of the shading box. When the original metal part is sent to the specified position, the CCD camera is triggered to capture the images while controlling different light units to turn on in a certain order. When the images are transmitted to the computer, the image analysis module is used to recover normal map and detect the image of metal parts. The proposed method for normal map reconstruction is described in detail in Section 3.

2.2 Image analysis for defect detection

The pipeline of the proposed defect detection framework is shown in Fig. 2(b). We have collected a lot of samples of positive and negative samples of the defects by sampling the images of normal and defected parts captured using our image acquisition system.

It should be noted that since most of the small surface scratches and noises are filtered out by the previous normal reconstruction module, the difficulty of defect detection can be reduced significantly. These samples are used to train a classifier by incorporating joint image features. With the trained classifier, we are able to process the image of each given part and find whether there are any defects on its surface. We will describe the method in Section 4.

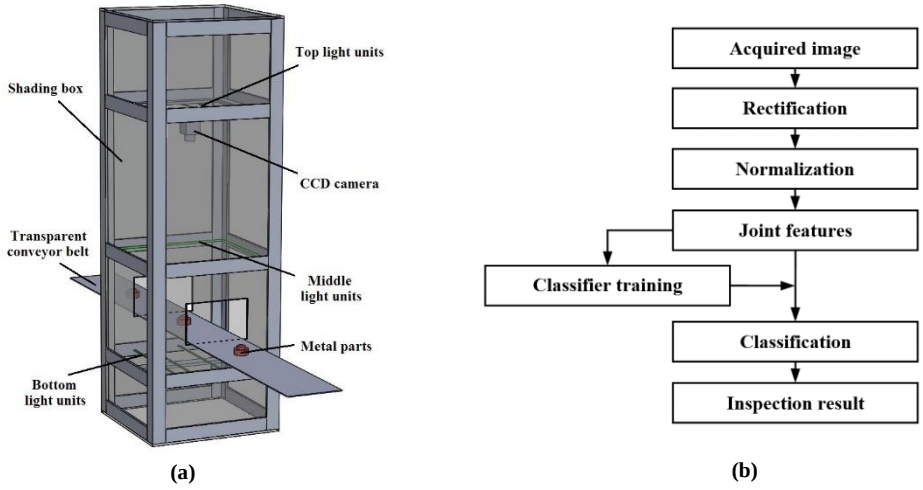

Fig. 2. (a) Image acquisition system (The shading box is rendered with semi-transparency to explain the interior structure of the system). (b) Pipeline of the defect detection framework.

3 Normal map reconstruction

As discussed previously, the acquired images are shown in Fig. 3. Intuitively, when the light unit in a certain direction opens, the imaged pixel is brighter if the local region around this pixel faces the lighting direction, and vice versa. The brightness of the image is only related to the slope angle of the material surface [10]. In view of this regularity, the normal maps can be recovered by the directional reflections of the parts.

A traditional method called direct calculation is calculating the directional images (north, south, east, and west) without light attenuation which is captured by the camera fixed on a slide. However, this method needs four slides, and the precise control of the light movement on the slides. So the equipment is too large and inconvenient to be manipulated, and overexposure is easy to appear because of the long exposure. To solve these problems, a novel method is proposed to calculate the light compensation of the directional images which is captured by a shading frame with combined light units. Compared with direct calculation, the proposed method is quite robust and effective to recover the normal map.

Firstly, a filter coating is installed on the camera, and then turn on the top, middle (four directions) and bottom light units in proper order, while taking pictures. Next, we

remove the filter coating and repeat the above steps. Based on the light compensation algorithms [10-12] and mixed superposition method in [13], the normal map of a part is reconstructed as shown in Fig.4. The main calculation steps are as follows:

Let *I_N1*, *I_S1*, *I_W1*, and *I_E1* indicate the filtered images in four directions, separately, according to a light compensation algorithm mentioned in [10], and store them separately as a single-channel floating point brightness map *I_NL*, *I_SL*, *I_WL*, *I_EL*. Next, creating two new three-channel images *NW* and *SE*, taking *I_WL* as R channel of *NW*, *I_NL* as G channel of *NW*, and adjust the color gradation of *NW* to 0~0.5. Taking *I_EL* as R channel of *SE*, *I_SL* as G channel of *SE*, and adjust the color gradation of *SE* to 0.5~1.0. Finally, *NW* and *SE* are blended to obtain image $N\_T1=2\times NW\times SE$. Because the normal information is a normalized vector, in this paper, it can further calculate the information of normal B channel based on the value of normal R and G channel. We assume the value of R channel is *r*, and the value of G channel is *g*, the value *b* of channel B is defined as $b = 2\times\sqrt{1-(r-0.5)^2-(g-0.5)^2}-1$.

Let *I_N2*, *I_S2*, *I_W2*, *I_E2* represent the unfiltered images in four directions, separately, and then calculating a normal map named *N_T2* by the same processing way. By the further processing including removing frilling, brightness adjustment, and contrast adjustment, the image *N_T1* and *N_T2* are transformed as the *normal1* and *normal2* respectively. The final normal map is blended by the *normal1* and *normal2* named as *Normal*, where $Normal = 0.5\times(normal1+normal2)$. The above normal map blending method is adopted to obtain a normal map which can retain the details of metal parts without color jump [13].

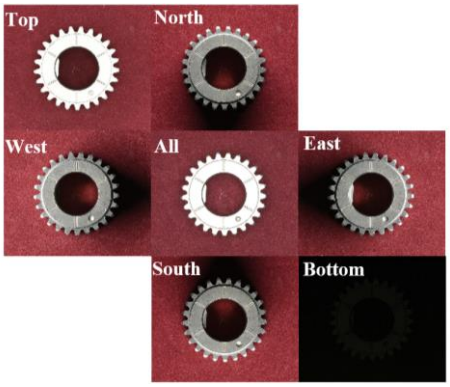

Fig. 3. Acquired images under the combined light units. (Top is meant to use only top light units. East is meant to use the eastern light units. All is meant to use all the light units)

4 Defect detection

For the convenience of detection, we firstly determine location and orientation of the acquired images, and then translate and rotate the normal maps of metal parts according to the positional relationship between the parts and a standard orientation. Besides, the

standard orientation contains the centroid and the angle between a straight line connecting the centroid with the anchor point and the horizontal axis. Finally, we extract the section of a part that needs to be detected. Specifically, about 90% of the background regions are filtered out by the image normalization which can speeds up the computation. The diagram of the normal information extraction is shown in Fig. 4.

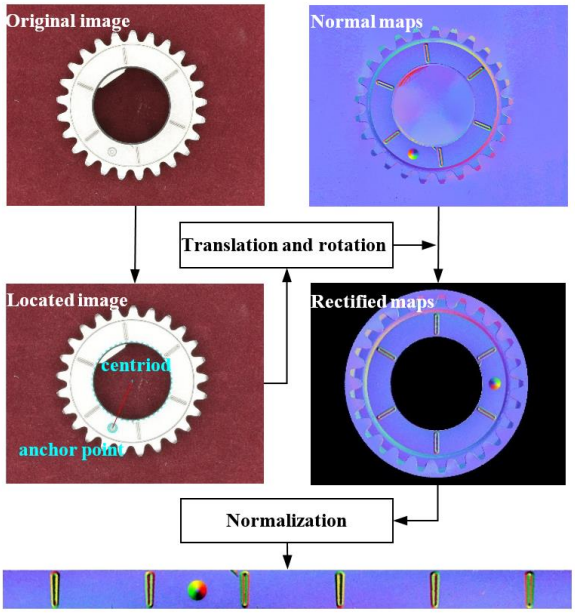

Fig. 4. Diagram of the normal information extraction.

After the processing of rectification and normalization, we use a cascaded classifier to identify whether there are any visual defects. The training of the cascaded classifiers includes joint features extraction, fast feature pyramid [14] and learning via the AdaBoost algorithm [15]. The classifier allows the non-defect areas to be quickly discarded while more computations are spent on the promising areas. The joint features are effective to capture the salient characteristics of the object. In this paper, the joint feature consists of four parts: LUV color features, rotation invariant local binary patterns (LBP), normalized gradient magnitude, and histogram of oriented gradients (HOG).

Fast feature pyramid can greatly accelerate the feature extraction speed without losing important information. Compared with the traditional method of computing image features step by step, fast feature pyramid only calculates a scale in each octave, and then use this feature to determine the other dimensions of image features within the octave. And the structure of the cascaded inspection process could essentially be considered as a degenerate decision tree. The initial stage classifier eliminates many non-defect images with little processing. After several stages of processing, the number of sub-windows is reduced rapidly. Finally, the sub-window that passes all stage classifiers is classified as a target (defect). Each stage classifier is composed of a set of weak

linear SVM classifiers and trained by the AdaBoost learning algorithm on labeled data.

5 Experimental results

To verify the performance of the proposed defect detection method, we present the experimental results followed the previous approaches on defect detection in this section. The experiment is developed under the PC condition 3.60GHz of Intel Core i7-7700 processor, 8G RAM and Nvidia GTX 1070ti.

5.1 Databases and evaluation metrics

In order to verify the effectiveness of the algorithm, we conduct an empirical study of evaluating the proposed detection method on a tiny surface defects database. The database contains 564 defected images and 3164 normal images, 70% of which are used for training. And all images are the size of 1200×900 pixels. Each training set image is labeled according to the format of the PASCAL VOC dataset [16]. To evaluate the effectiveness of the proposed method, there are four indexes [17]: correct detection rate (CDR), missing detection rate (MDR), false detection rate (FDR), and detection speed. For example, if a testing set contains m defect images and n non-defect images, by detection of the method, a images are inspected as defect, among them b images are inspected by error, meanwhile, c images are inspected as non-defect, among them d images are inspected by error. So, the above indexes can be defined as: CDR = $1-b/(m+n)$, MDR = $b/(m+n)$, FDR = $d/(m+n)$. In the task of the defect detection, the index of FDR is less crucial than MDR, because the impact is not serious if a non-defect region is detected by error.

5.2 Comparison of different images from combined light units

To observe the influences of images under different light units, we compare our method in different images from combined light units. Fig. 5 shows typical detection results. The results show that our method can effectively detect and recognize the defect based on the normal map. The Top image usually contains highlight information. So our method can be easily affected by the serious interference of surface reflection on metal parts. In addition, the directional images present too many small surface scratches in details. The detection method can be easily affected by the noise and small surface scratches of metal parts. In conclusion, the normal map can ensure high detection accuracy of the tiny surface defects of small ring parts.

5.3 Performance comparison with the related methods

To illustrate the superiority of proposed method for defect detection, we also carry out experiments using hand-crafted feature descriptors and conventional machine learning tools. With some widely used object detection methods such as cascade detector [18] based on Haar-like and HOG, the gradient coded co-occurrence matrix (GCCM) [19]

and the deep learning method based on convolutional neural network (CNN) [20, 21], the same images are trained for defect detection. The other parameters are all default values. The detection results are detailed in Tables 1. Our method has 99.15% CDR, 0.85% MDR, and 4.00% FDR. The proposed detection method outperforms other related methods based on normal maps. Some typical results are shown in Figs. 6 to 8. Our method can be effectively applied to the detection of tiny surface defects.

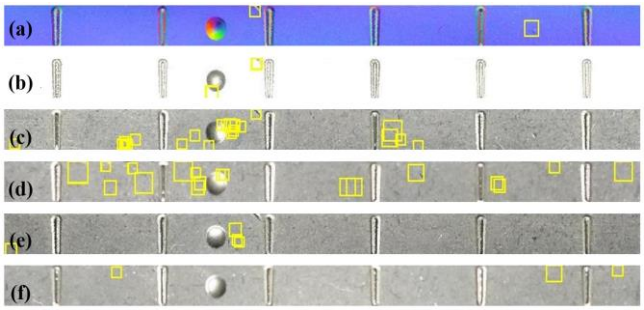

Fig. 5. Detection results of different images from combined light units. (a) Normal. (b) Top. (c) East. (d) West. (e) South. (f) North

Table 1 also lists a comparison of the detection speed. the computation speed of the cascade of Haar-like features method is the fastest, but its accuracy is the lowest. The accuracy of the CNN-based method is satisfactory, but its speed is too low because of the computational complexity of CNN. In addition, CNN-based method cannot effectively deal with detection of tiny surface defects. The results confirm that our method is preferable for the visual detection framework.

Table 1. Detection results of different methods.

Methods	CDR/%	MDR/%	FDR/%	Speed/ms
Cascade(Haar-like)	81.20	9.80	23.93	**11**
Cascade(HOG)	92.31	7.69	12.82	17
GCCM	89.74	10.26	19.66	586
CNN-based	96.43	3.56	17.86	168
Our method	**99.15**	**0.85**	**4.00**	23

There are three main reasons that make the visual detection framework have high inspection accuracy and speed. First, the cascaded detection approach is important to make the framework fast, which allows background regions of the image to be quickly discarded while spending more computation on promising regions. Second, image normalization technology significantly speeds up the computation. Specifically, about 90% of the background regions are filtered out by image normalization, and only 10% of the image regions need to be verified in the following module. Third, the joint features are effective to capture the salient characteristics of the defects.

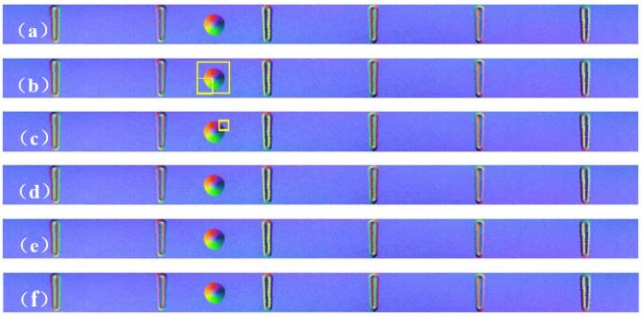

Fig. 6. Detection results of different methods. (a) Ground truth. (b) Cascaded detector with Haar-like. (c) Cascaded detector with HOG. (d) GCCM. (e) CNN-based. (f) Our method.

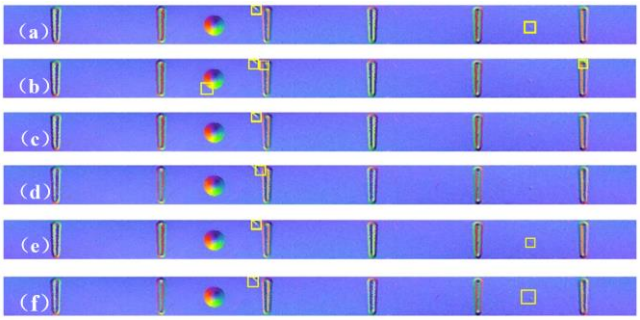

Fig. 7. Detection results of different methods. (a) Ground truth. (b) Cascaded detector with Haar-like. (c) Cascaded detector with HOG. (d) GCCM. (e) CNN-based. (f) Our method.

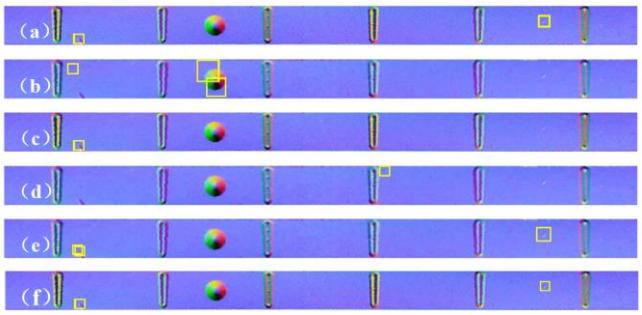

Fig. 8. Detection results of different methods. (a) Ground truth. (b) Cascaded detector with Haar-like. (c) Cascaded detector with HOG. (d) GCCM. (e) CNN-based. (f) Our method.

6 Conclusion

In this paper, a novel visual method is proposed to detect tiny surface defects of the small metal parts under interference of small surface scratches. Unlike the conventional

methods, the proposed method can achieve a high detection rate based on the normal maps of metal parts. And the joint features are used to train an accurate and effective detector by the Adaboost approach and fast feature pyramid. The results show that the approach outperforms other methods with a significantly fast speed only 23 milliseconds per mechanical part. For the future work, an extended version of our method could be used to detect a greater variety of metal parts with a higher accuracy.

Acknowledgments. This work is supported in part by the Natural Science Foundation of Jiangsu Province under Grants BK20150016, the National Natural Science Foundation of China under Grants 61772257, 61672279, and the Fundamental Research Funds for the Central Universities 020214380042.

References

1. Senthikumar, M., Palanisamy, V., Jaya, J.: Metal surface defect detection using iterative thresholding technique. In: Proceedings of International Conference on Current Trends in Engineering and Technology, pp. 561-564 (2014)
2. Kandroodi, M. R., Araabi, B. N., Bassiri, M. M., Ahmadabadi, M. N.: Estimation of depth and length of defects from magnetic flux leakage measurements: verification with simulations, experiments, and pigging data. IEEE Trans. Magn. **53**(3), 1-10 (2017)
3. Hui, L., Zheng, B., Wang, Z. B., Guo, H. L.: Numerical simulation of laser ultrasonic transmitted wave: applied to detect surface defects depth. J. North Univ. China **38**(2), 119-123 (2017)
4. Wang, Y., Yao, W., Liu, H., Guo, H.: An experimental study on depth evaluation of micro-surface crack by laser generated acoustic surface waves. J. Appl. Acoust. **35**(1), 36-40 (2016)
5. Yang, R., Zhang, H., Li, T., He, Y.: An investigation and review into microwave thermography for NDT and SHM. In: Proceedings of Ndt New Technology and Application Forum, pp. 133-137, (2016)
6. Dudzik, S.: Analysis of the accuracy of a neural algorithm for defect depth estimation using PCA processing from active thermography data. Infrared Phys. Technol. **56**(36), 1-7 (2013)
7. Bernieri, A., Betta, G., Ferrigno, L., Laracca, M.: Crack depth estimation by using a multi-frequency ECT method. IEEE Trans. Instrum. Meas. **62**(3) 544-552 (2013)
8. Faghih-Roohi, S., Hajizadeh, S., Núñez, A., et al.: Deep convolutional neural networks for detection of rail surface defects. In: Proceedings of International Joint Conference on Neural Networks, pp. 2584-2589 (2016)
9. Edris, M. Z. B., Jawad, M. S., Zakaria, Z.: Surface defect detection and neural network recognition of automotive body panels. In: Proceedings of International Conference on Control System, Computing and Engineering, pp. 117-122 (2016)
10. Aittala, M., Weyrich, T., Lehtinen, J.: Two-shot SVBRDF capture for stationary materials. ACM Trans. Graph. **34**(4), 1-13 (2015)
11. Jian, M., Lam, K. M., Dong, J.: Illumination-insensitive texture discrimination based on illumination compensation and enhancement. Inform. Sciences **269**(11), 60-72 (2014)
12. Jian, M., Yin, Y., Dong, J., et al.: Comprehensive assessment of non-uniform illumination for 3D heightmap reconstruction in outdoor environments. Comput. Ind. **99**, 110-118 (2018)
13. Lv, G. J.: Material Surface Visualization and its Application. M.S. thesis, Dept. Comput. Sci., Nanjing University, China, 2017.

14. Dollar, P., Appel, R., Belongie, S., Perona, P.: Fast feature pyramids for object detection. IEEE Trans. Pattern Anal. Mach. Intell. **36**(8), 1532-1545 (2014)
15. Nam, W., Dollar, P., Han, J. H.: Local decorrelation for improved pedestrian detection. In: Proceedings of Advances in Neural Information Processing Systems, pp. 424-432 (2014)
16. Everingham, M., Eslami, S. M. A., Gool, L. V., et al.: The pascal visual object classes challenge: a retrospective. Int. J. Comput. Vision **111**(1), 98-136 (2015)
17. Zhang, Y., Lin, K., Zhang, H., et al.: A unified framework for fault detection of freight train images under complex environment, In: Proceedings of IEEE International Conference on Image Processing, (2018)
18. Viola, P., Jones, M. J.: Rapid object detection using a boosted cascade of simple features. In: Proceedings of Computer Vision and Pattern Recognition, pp. 511-518 (2001).
19. Liu, L., Zhou, F., He, Y.: Automated visual inspection system for bogie block key under complex freight train environment. IEEE Trans. Instrum. Meas. **65**(1), 1-13 (2015)
20. Krizhevsky, A., Sutskever, I., Hinton, G. E.: ImageNet classification with deep convolutional neural networks. In: Proceedings of International Conference on Neural Information Processing Systems, pp. 1097-1105 (2012)
21. Simonyan, K., Zisserman, A.: Very deep convolutional networks for large-scale image recognition. In: Proceedings of International Conference on Learning Representations, (2015)